ELSEVIER

Ceramics International 26 (2000) 325–335

CERAMICS INTERNATIONAL

Electrical resistivity of ceramic–metal composite materials: application in crucibles for induction furnaces

J.R. Martinelli*, F.F. Sene

Energy and Nuclear Research Institute, Brazilian Nuclear Energy Commission, C.P. 11049 - Pinheiros, 05422-970 S. Paulo, SP, Brazil

Received 2 March 1999; received in revised form 9 March 1999; accepted 5 May 1999

Abstract

A study was conducted of the electrical properties of partially-stabilized zirconia ceramic matrix composites with 0 to 40 vol% of titanium, niobium, nickel, and titanium and cristobalite, over temperatures ranging from 25 to 800°C. Composites containing metallic inclusions above 25 vol% show the predominance of electronic type conduction. For metallic inclusions bellow 25 vol%, a typical ionic conduction behavior has been observed. Due to the percolation effect, partially-stabilized zirconia containing 25 vol% of titanium, or nickel, shows an insulator to conductor transition, and cristobalite containing 30 vol% of titanium shows a conductor to insulator transition as the temperature is raised. Crucibles of composites of partially stabilized zirconia containing titanium were made by slip casting and sintering. Tests performed in an induction furnace showed that both pellets and crucibles containing metallic inclusions above 25 vol% had self-heated. The maximum temperature reached by fixing the power to 2 kw was 1350°C without any charge. X-ray diffraction, energy dispersive spectroscopy, scanning electron and optical microscopy were performed to provide a full microstructure characterization. Continuous paths formed by metallic clusters can be seen for materials containing metallic concentration over 25 vol%.

Keywords: B. Composites; C. Electrical conductivity; D. ZrO_2

1. Introduction

The addition of ceramic particles to metals has been done since the thirties in order to improve the mechanical properties of metal alloys. For instance, tungsten carbide was added to cobalt, and consequently this *cermet* could be used as cutting tools [1]. Recently, metal alloys and ceramic materials have been reinforced with ceramic particles and whiskers in order to improve their mechanical properties too. These materials have been named composites, and they are attractive to be used as structural materials because of their relatively low density, high toughness, and improved mechanical strength [2].

Electrical properties of composite materials are also relevant and should be investigated more extensively, which could lead to a wide range of applications. One of the main phenomenon to be investigated is the insulating to conducting transition that happens in a narrow percolation range. This phenomenon depends on the concentration, shape, dimension and crystallographic direction of the embedded particles.

The increase of the electrical conductivity of insulating materials containing metallic inclusions during the exposition to electromagnetic fields was first reported by Brandy in 1890. New electrical conducting paths were observed when materials were exposed to radio frequency fields. Those paths were responsible for a drastic increase of the conductivity.

Composite materials that combine insulating and conducting phases are similar to the ones studied by Brandy.

Electrical properties have been previously measured at room temperature for ceramic–metal composites such as Al_2O_3–Ti [3], ZrO_2–TiCN [4], ZrO_2–Ti and ZrO_2–Nb [5]. Generally, a reduction of electrical resistivity has been observed as the concentration of metallic inclusions is raised.

Zirconia has been used in high temperature applications (> 1000°C) due to its high melting point and chemical inertness. Zirconia is used as heating elements, cathodes for plasma torches and electrodes for MHD

* Corresponding author. Tel.: +55-11-816-9346; fax: +55-11-816-9370.

E-mail address: jroberto@net.ipen.br (J.R. Martinelli).

0272-8842/00/$20.00
PII: S0272-8842(99)00059-0

energy conversion. Furthermore, partially- stabilized zirconia (PSZ) is extensively used as oxygen sensors and as electrodes in H_2 production devices based on the thermohydrolysis of water [6].

Composite materials based on insulating matrix and conducting inclusions can be potentially used in a wide range of technological applications such as in the manufacture of crucibles for vacuum induction furnaces. Crucibles made of carbon free materials can be used in melting processes that require no carbon contamination. Thermal etching of ceramic materials can also be performed by using composite materials in this same heating process. When composite materials show electrical resistivity behavior with positive temperature coefficient, devices sensible to temperature variation can be built [7]. If the material shows non-linear current–voltage behavior in the percolation region, varistors can be produced [8]. Finally, electrodes for fuel cells made by zirconia–Ni have been reported [9].

In the present work the mechanisms of electrical conduction in PSZ–Ti, PSZ–Nb, PSZ–Ni were investigated through the measurement of electrical resistivity as a function of temperature. It was also checked the self-heating behavior of these materials when exposed to electromagnetic fields in the range of radio frequency (r.f.). The system α-SiO_2–Ti was also investigated because cristobalite shows a relatively low temperature phase transition with volume change which can provide some information on percolation related to phase transition. Crucibles made of ZrO_2–Ti by slip casting were checked in an induction furnace for self heating.

2. Experimental procedure

Partial stabilized zirconia containing 3 mol% of ytria was prepared by coprecipitation of zirconium hydroxide from an aqueous solution of $ZrOCl_2$ and YCl_3. Ammonium hydroxide was used as the precipitation agent. The precipitated material was filtered, washed in distilled water, dehydrated in ethyl alcohol, washed with acetone, filtered again and finally dried at 100°C for 24 h. The material was then calcined in air at 850°C for 2 h, ground in a mortar with a pestle and finally ball milled with alumina media for 3 h. Impurity levels for all raw materials were determined by flame spectroscopy. A spectrograph Jarrel model S 800 was used for that purpose.

The particle size distribution was determined by using a sedigraph Micromeritics Model 5100. The yttrium oxide molar fraction in the PSZ after the coprecipitation process was determined by X-ray fluorescence. The PSZ tetragonal phase content and the amount of all other crystalline phases were determined by X-ray diffraction. A Rigaku Model DMAX-100 diffractometer was used for this purpose. The amount of monoclinic and tetragonal zirconia phases were determined from the appropriated X-ray diffraction peak intensities [10].

Mixtures of PSZ with Nb, Ti, or Ni powders in the range of 10 to 45 vol% were used to prepare 14 mm diameter pellets by uniaxial pressing at 100 MPa for 15 s. Pellets of cristobalite–Ti were also prepared following the same procedure. These pellets were finally isostatically pressed at 200 MPa for 60 s at room temperature.

Samples of PSZ–Nb and PSZ–Ti were sintered in a tubular electric furnace in argon at 1600°C for 1.5 h. The heating rate was 10°C/min. To sinter PSZ–Ni and SiO_2–Ni pellets the same procedure was adopted except for the sintering temperature that was 1450°C.

Densities for all samples before and after sintering were determined by the Archimedes' method.

Microstructure characterization was performed by using a light microscope Olimpus and a scanning electron microscope Philips Model XL30 with capacity for energy-dispersive X-ray spectroscopy. Samples were prepared by cutting and polishing with diamond pastes from 15 to 1 μm. A thermal etching was performed on PSZ samples containing Ti or Nb at 1500°C for 20 min in argon in order to reveal the grain boundaries. Samples were finally coated with gold by sputtering before performing the SEM analyses.

A preliminary electrical evaluation of the samples was performed at room temperature in order to classify them as insulators or conductors. A multimeter Fluke model 8050A and an electrometer Keithley model 610C were used to measure the electrical resistance of these samples.

Electrical resistivity measurements in the temperature range of 25–800°C under argon flow of 1 l/min were also performed on samples 2 to 5 mm thick by using the two probe d.c. method. Electrodes were built on the sample surfaces by previously coating them with platinum by sputtering. Fig. 1 shows a schematic diagram of the experimental setup. A thermocouple was set close to the sample to provide a precise temperature measurement. Platinum wires were used to connect the electrodes to the electrometer. A reversible switch was used to reverse the electrodes and consequently to eliminate any artifact caused by parasitic currents due to thermal gradients.

Composite materials were exposed to r.f. and the temperature was measured as a function of power and voltage of the r.f. generator. An induction furnace HWG was used for that purpose. Temperatures were measured by a pyrometer Minolta model S40. The experimental setup is described elsewhere [11].

Crucibles of PSZ containing 10–30 vol% of Ti were made by slip casting. Powders of Ti and PSZ were mixed in water. A commercial product named Lambra was added as deflocculator. A mold made of plaster of Paris was used to cast the slurry in the shape of crucibles.

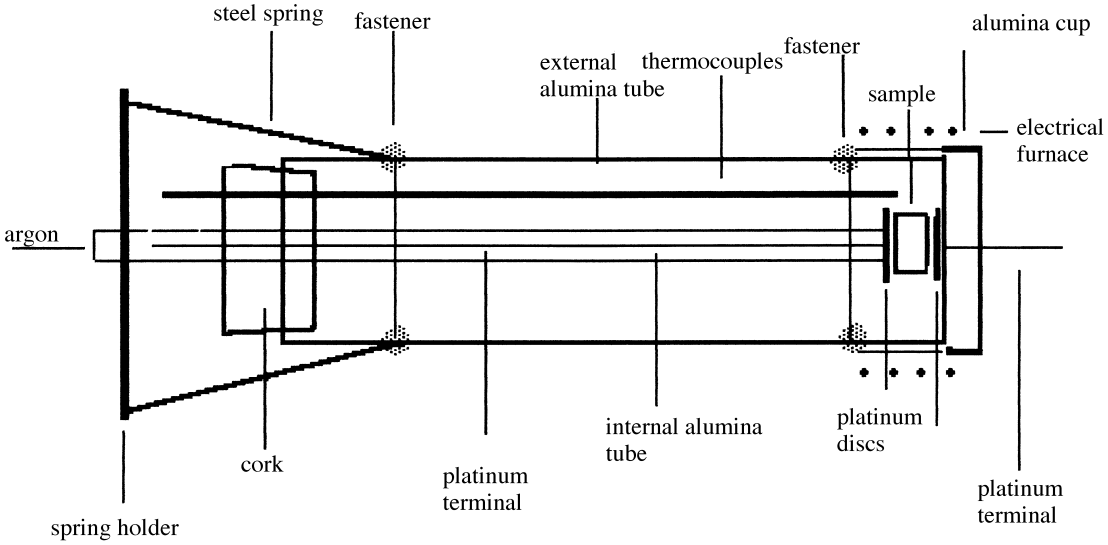

Fig. 1. Experimental arrangement for measurement of electrical resistivity as a function of temperature.

The material was pulled out from the mold, dried at 100°C for 24 h, pre-sintered at 1000°C in argon for 1 h, polished and finally sintered in argon at 1600°C for 1.5 h. These crucibles were also exposed to r.f. and the temperature was monitored following the same procedure described above.

3. Results and discussion

Table 1 shows the main impurities in the raw materials. Aluminum and silicon in PSZ are originated from the milling process. A relatively high concentration of Ta is found in Nb powders. It is quite difficult to remove Ta from Nb during the purification process. However, we believe that these impurities will not substantially affect the percolation of electrical paths in our composite materials when compared to the effects expected by metallic inclusions. In fact, impurities could change the electrical resistivity background. Others factors, such as metal particle oxidation and the contact geometry would far overshadow the effects due to impurities in the metal phase.

The molar fraction of yttria in PSZ was determined to be 2.8 mol%, which is enough to keep the zirconia partially stabilized. From the X-ray diffraction the tetragonal phase content was determined to be 96.4%.

Fig. 2 shows a representative example of X-ray diffraction patterns for PSZ–10 vol% Nb, and for SiO_2–10 vol% Ti after sintering. Others diffraction patterns show similar characteristics related to the material's constituents. Diffraction peaks related to the metallic inclusions and ceramic matrix are also shown. From the diffraction patterns it was possible to calculate the amount of crystalline phases shown in Table 2.

The medium equivalent spherical diameters for PSZ, cristobalite, Nb, Ti, and Ni are 2.8, 9, 35, 38, and 25 μm, respectively. It is noticed that the metallic particle average sizes are one order of magnitude higher than the ceramic ones. Therefore it can be assumed that mixtures of ceramic and metal particles described in the present work are suitable for the preparation of ceramic–metal composites, since the probability to have metallic inclusions inside ceramic grains will be low [12].

In order to compare the composite density to a reference value, the rule of mixture was used to calculate the "theoretical" density value (TD) considering the volumetric

Table 1
Impurities detected by flame spectroscopy for: PSZ, niobium, titanium, nickel, and cristobalite (μg/g)

Element	PSZ	Nb	Ti	Ni	α-SiO_2
Fe	40	3	6	75	75
Cr	10	6	300	45	45
Ni	2	6	150	–	45
Zn	20	200	9	150	150
Si	160	8	9	60	
Al	20	3	300	60	200
Mn	1	2	10	20	20
Mg	100	6	10	45	45
Pb	2	6	9	45	45
Sn	2	4	6	30	30
Bi	2	2	6	15	15
Cu	5	–	9	45	45
Na	30	–	–		–
Ba	–	–	–	150	150
Co	–	6	–	45	45
Ca	–	3	20	75	75
Sb	–	–	–	45	45
V		100	9	30	30
Ta		13 000	–		–
Ti				45	–

fractions of metallic inclusions and the ceramic matrix. Density for green samples varied from 57 to 62% TD and for sintered samples, from 72 to 92% TD depending on the volume and type of metallic inclusions. The density after sintering decreases as the amount of metallic inclusions is raised. This result is in agreement with the theoretical model that explains the densification of ceramic materials in the presence of embedded metallic particles, considering the difference between the ceramic and metal sintering rates, and the relatively low diffusion of their constituents [12]. In the other hand density of green samples increases as the amount of metallic inclusions is raised. Metal particle inclusions lead to higher ductility and mechanical deformation during the compaction.

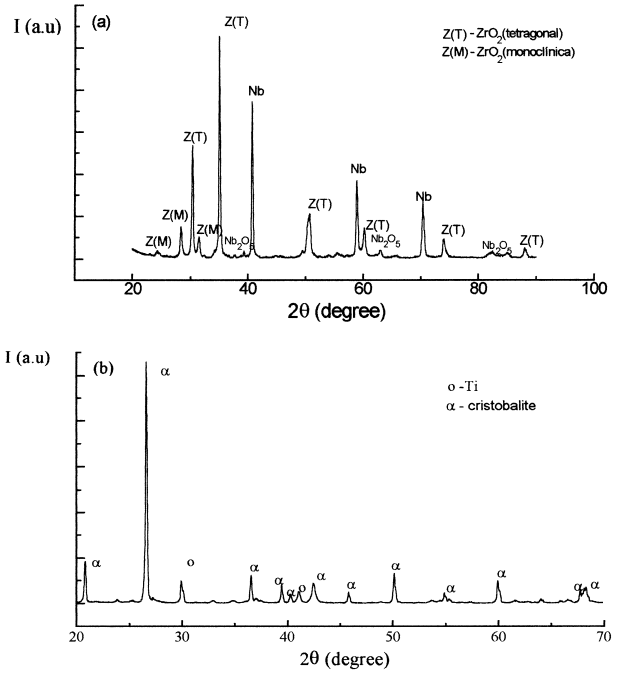

Fig. 2. X-ray diffraction patterns for: (a) PSZ–10 vol% Nb, and (b) SiO_2–10 vol% Ti.

Table 2
Amount of detected phases in the sintered samples: (a) PSZ–Ti, (b) PSZ–Nb, (c) PSZ–Ni and (d) SiO_2–Ti

Phase	Amount (%vol)	Phase	Amount (%vol)
a. *PSZ–Ti*		b. *PSZ–Nb*	
ZrO_2(T)	92.0	ZrO_2(T)	85.0
ZrO_2(M)	0.2	ZrO_2(M)	4.2
Ti	7.5	Nb	9.0
TiO_2	<1.0	Nb_2O_5	<1.0
c. *PSZ–Ni*		d. *SiO_2–Ti*	
ZrO_2(T)	89.0	SiO_2(α)	92.0
ZrO_2(M)	0.2	Ti	7.5
Ni	9.4	TiO_2	–
NiO	–	–	–

4. Microstructure analyses

Fig. 3 shows the microstructure of PSZ–10Ti, PSZ–20Ti, PSZ–30Ti and PSZ–45Ti samples taken from a light microscope (LM).

The metallic inclusions are located in the white regions and the ceramic matrix is the gray region in those pictures. Pores are represented by black spots. From Fig. 3A and B (samples that are insulators at room temperature) it can be noticed that there is an increase of metallic inclusions without formation of continuous paths. In Fig. 3C (sample that shows electrical conduction at room temperature) few continuous paths can be seen formed by metallic clusters. In the sample showed by the Fig. 3D (electrical conductor sample) these paths are saturated. Samples containing niobium and nickel show similar microstructure characteristics.

Fig. 4 shows a microstructure from PSZ–Ti and PSZ–Nb obtained by SEM. By comparing the Nb and Ti dot mapping built by EDS and the microstructures of corresponding samples, it is quite possible to assume that most of the metallic inclusions are located at the grain boundaries. Few metallic grain clusters have been observed . The amount of clusters increases as the metallic particle inclusion is raised. When these clusters touch themselves electronic conduction paths are formed. The ceramic grain medium size is 30 ± 5 μm and it does not depend on the amount of Nb and Ti. The porosity of the material increases as the metal particle amount is raised leading to lower density values as it was earlier reported.

5. Electrical properties

A typical electrical behavior of composite materials containing metallic particles embedded in a ceramic matrix is shown in Fig. 5. The electrical resistivity is plotted as a function of Ni concentration in a PSZ matrix. As the amount of metal inclusion is raised, the originally insulating material becomes conductor. The critical Ni volumetric fraction is $28 \pm 2\%$. This result is in agreement with the percolation model established by Landauer [13]. All other materials investigated in this work show a similar electrical behavior.

Fig. 6 shows the electrical resistivity as a function of temperature for PSZ–Ti, PSZ–Nb, PSZ–Ni, and αSiO_2–Ti containing 30 vol% of metallic inclusions. The electrical resistivity increases linearly showing that the electrical conduction is electronic type and probably it will occur through the metallic conduction paths. The electrical resistivity of these composites are three orders of magnitude higher than the ones related to pure metals. This difference is probably caused by impurities in the metal crystalline lattice, the cross section and length of

conducting paths, which were not determined in the present work. As it is known, some metal alloys show resistivity values up to three orders of magnitude higher then pure metals [14]. Moreover, other factors can contribute in the reduction of electrical conductivity such as reduced contact area among conducting particles due to oxidation.

Fig. 7 shows the electrical resistivity as a function of temperature in an Arrhenius plot for PSZ samples containing 10 and 20 vol% of Nb. The activation energies are 0.78 and 0.72 eV, respectively. The electrical resistivity of these samples, originally insulators at room temperature, decreases exponentially as the temperature is raised. The conduction mechanism is similar to the one established for pure PSZ, but the activation energy (E_a) and the pre-exponential factor are different [15]. The conduction is primarily ionic and occurs through the PSZ matrix.

The PSZ–Nb composites show higher resistivity values than pure PSZ and this fact can be explain if it is considered that Zr^{+4} ions are replaced by Nb^{+5} in the PSZ lattice. To keep the electrical neutrality, each positive charge originated from the aliovalent ion in the lattice should be compensated by an electron and an oxygen atom. The electron will contribute for the electronic conduction but the oxygen atom will occupy an oxygen vacancy usually located in the lattice of a non-stoichiometric oxide, leading to higher resistivities.

On the other hand a lower value for the activation energy has been observed in the PSZ–Nb, therefore it can be assumed that the mobility of oxygen ions is higher. The charge carrier mobility depends on the ceramic microstructure and the existence of grain boundaries leads to an increase of mobility. Niobium inclusions can lead to microstructure defects [16]. However the d.c. electrical measurements do not allow to separate grain boundary from bulk effects.

Eq. (1) shows the electrical balance due to the replacement of Zr^{+4} by Nb^{+5}.

$$2Nb_{Nb}5O_O \longleftrightarrow 2Nb_{Zr}^{\cdot} + 4O_O + V_{Nb}' + \tfrac{1}{2}O_2 \qquad (1)$$

Therefore, as a consequence of this neutrality, niobium vacancy and oxygen atoms are generated.

Fig. 8 shows the electrical resistivity as a function of temperature in an Arrhenius plot for PSZ samples containing 10 and 20 vol% of Ti. The activation energies are 0.98 and 0.93, respectively.

These values are close to the ones for pure PSZ. The ion Ti^{+4} has a similar valence compared to zirconium in the PSZ lattice, and even if a replacement of Zr^{+4} by Ti^{+4} happens, there is no electrical unbalance in the

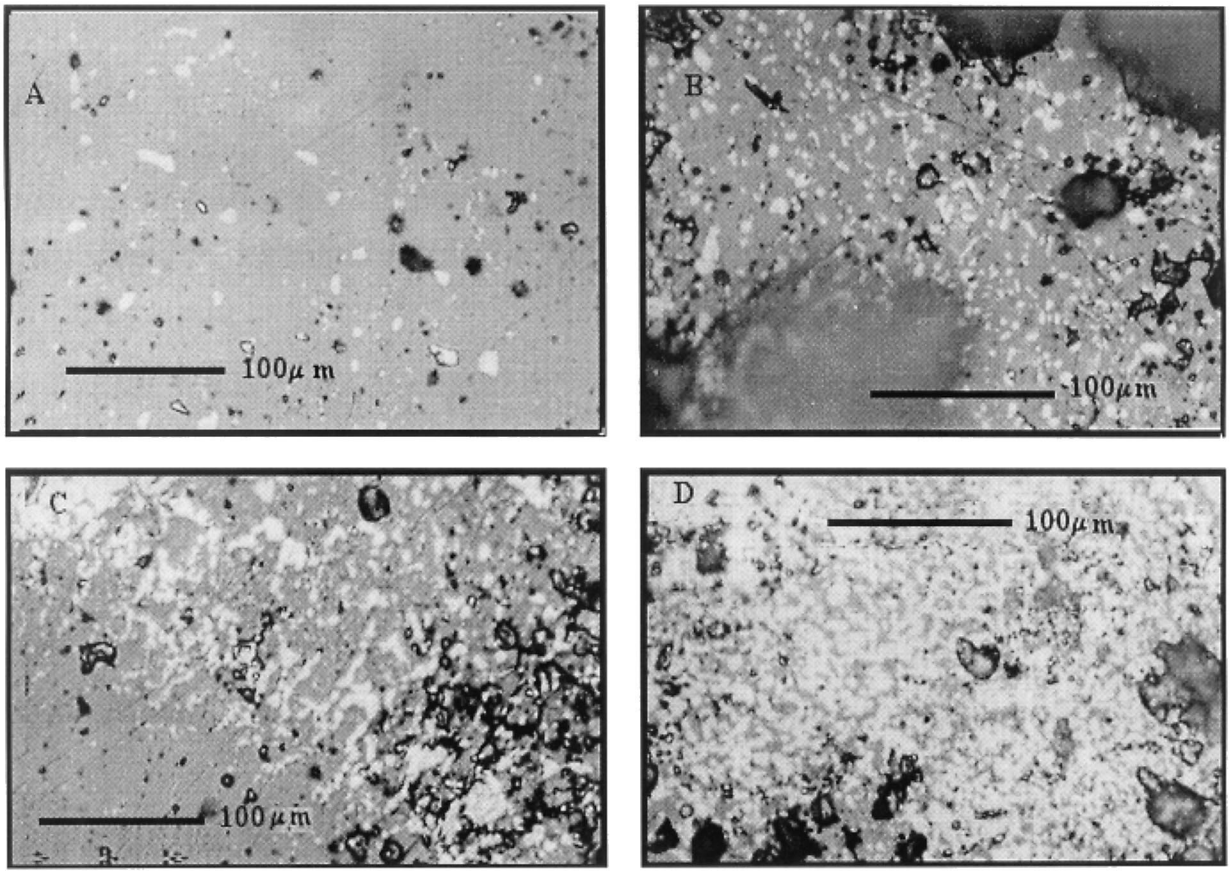

Fig. 3. Micrographical pictures taken by an optical microscope for: (A) PSZ–Ti 10; (B) PSZ–Ti 20; (C) PSZ–Ti 30; and (D) PSZ–Ti 45.

crystalline lattice, so no defects are generated to keep the electrical neutrality.

Fig. 9 shows the electrical resistivity as a function of temperature in an Arrhenius plot for PSZ samples containing 10 and 20 vol% of Ni. The activation energies are 1.00 and 0.98 eV, respectively.

The resistivity of PSZ–Ni is lower than the one for pure PSZ, and this fact can be explained considering that Zr^{+4} in the PSZ lattice is replaced by Ni^{+2}. To keep the electrical neutrality, a doubly ionized oxygen vacancy is formed. The ion mobility in this material is similar to the one expected for the nominally pure PSZ. The following equation shows the electrical charge balance corresponding to the replacement of Zr^{+4} by Ni^{+2}:

$$Ni_{Ni}O_O \longleftrightarrow Ni'''_{Zr} + O_O + V^{\bullet\bullet}_O \quad (2)$$

Fig. 10 shows the electrical resistivity of cristobalite nominally pure and containing 20 vol% Ti as a function of temperature in an Arrhenius plot. The activation energies are 0.73 and 0.64 eV, respectively.

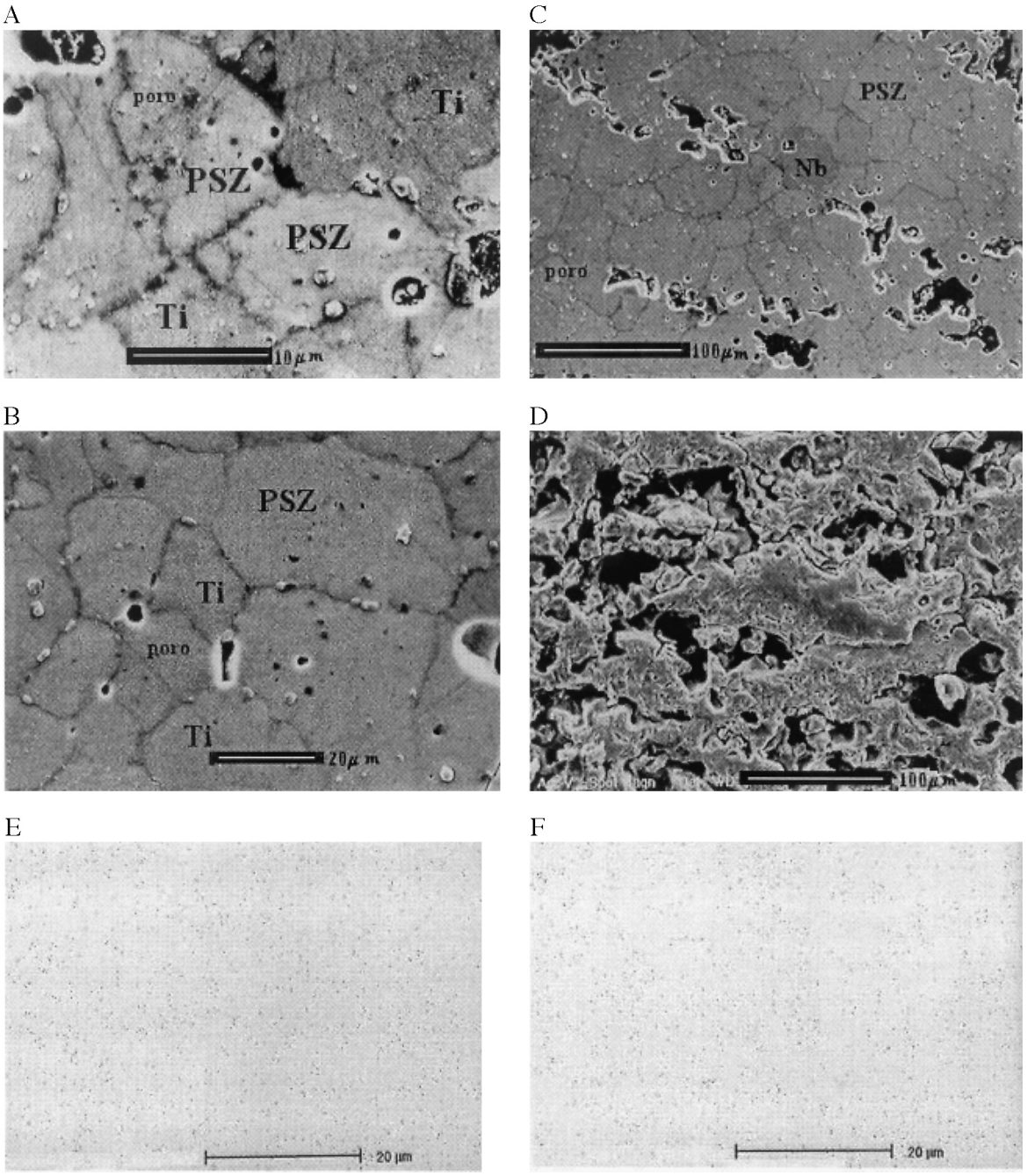

Fig. 4. Micrographical pictures taken by SEM for: (A) PSZ–Ti 10; (B) PSZ–Ti 30; (C) PSZ–Nb 10; (D) PSZ–Nb 45; (E) PSZ–Ti 10 (mapping by EDS for Ti); and (F) PSZ–Nb 10 (mapping by EDS for Nb).

In the case of cristobalite–Ti, it can be assumed that the conduction mechanisms are similar to the ones shown by the PSZ–Ti, considering that the valences of Ti and Si are equal and if Si is replaced by Ti in the cristobalite crystalline lattice, there is no need of point defects to keep the electrical neutrality.

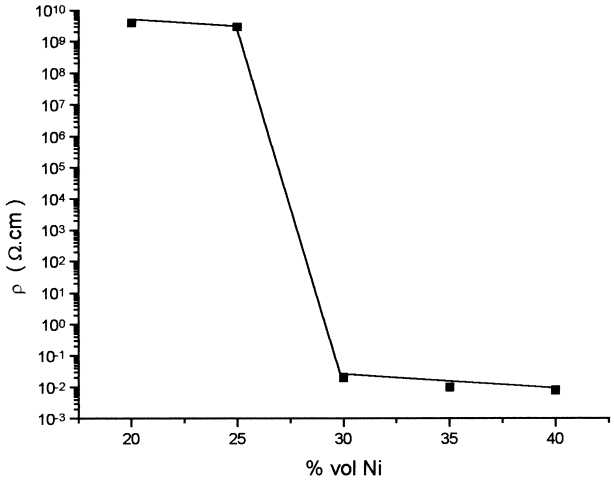

Fig. 5. Electrical resistivity as a function of nickel concentration.

Fig. 11a and b shows the electrical resistivity as a function of temperature for PSZ containing 25 vol% Ti and Ni, respectively.

As can be seen from these figures there are three distinct regions related to the electrical resistivity behavior. In region I the resistivity decreases exponentially as the temperature is raised. The activation energies in this region are 0.89 and 0.96 eV for PSZ–Ti and PSZ–Ni, respectively. The conduction mechanisms are similar to the ones related to PSZ containing 10 and 20 vol% of Ti and Ni, respectively. In region II a sharp transition occurs which is typical of a percolation process. In region III the resistivity is practically unchanged.

The Landauer's percolation model expresses the electrical conductivity as a function of the variation of the volumetric fraction for each component. For composite materials built by components with different thermal expansion coefficients or that show phase transitions, the percolation phenomenon can be induced by the temperature variation. A volumetric fraction change caused by different expansion coefficients can lead to the percolation region, mainly if there are some space available among metal particles to allow their expansion, as it is the present case since a 20 vol% porosity is

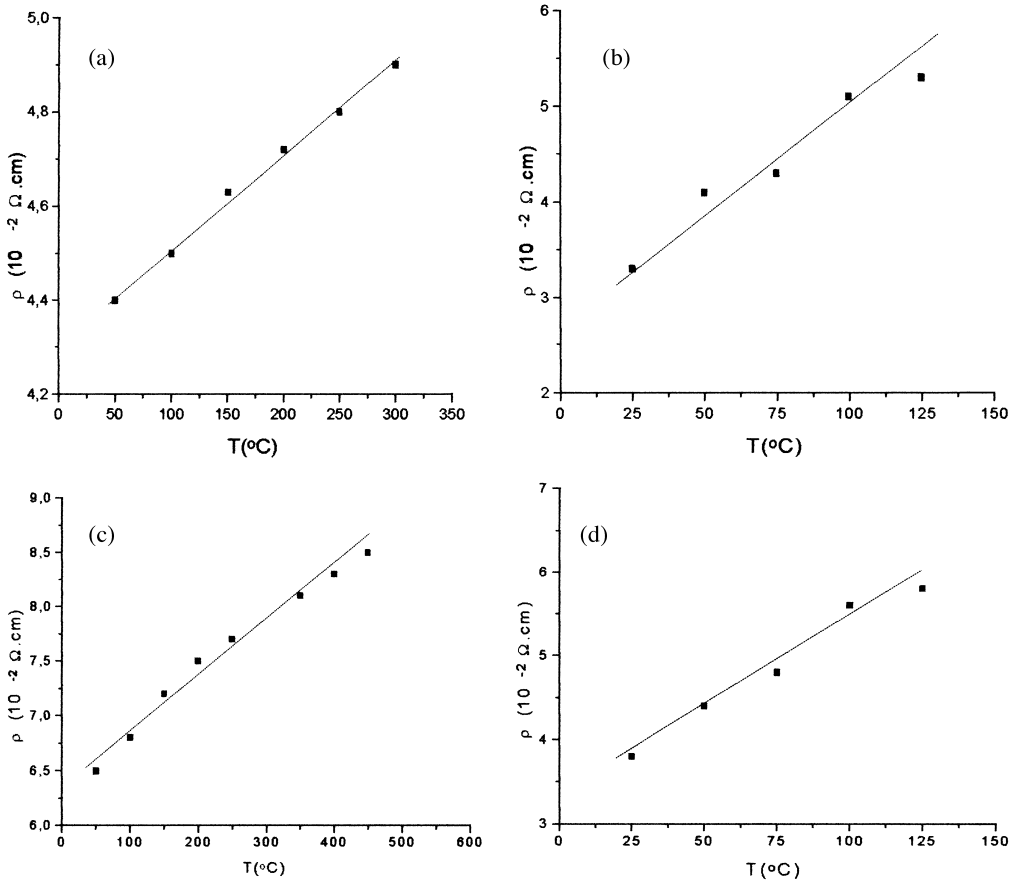

Fig. 6. Electrical resistivity as a function of temperature for: (A) PSZ–Nb (30 vol%); (B) PSZ–Ti (30 vol%); (C) PSZ–Ni (30 vol%); and (D) cristobalite–Ti (30 vol%).

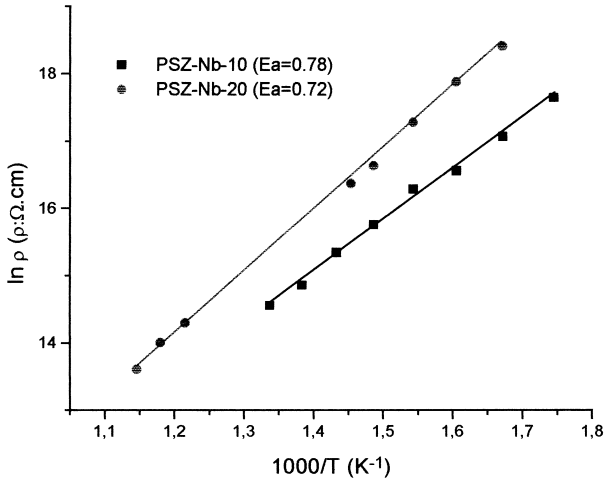

Fig. 7. Electrical resistivity as a function of temperature for PSZ samples containing Nb.

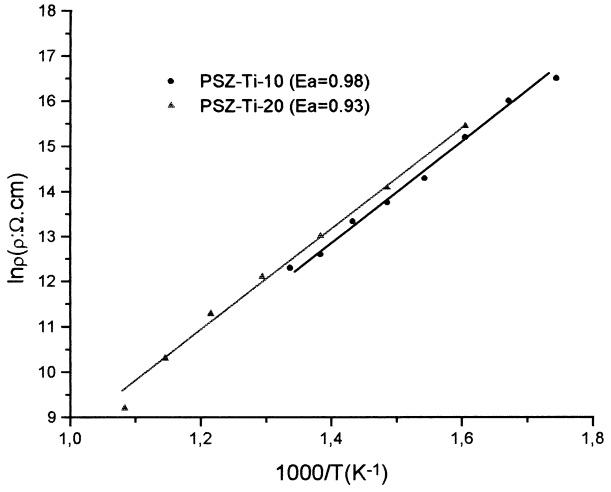

Fig. 8. Electrical resistivity as a function of temperature for PSZ–Ti samples.

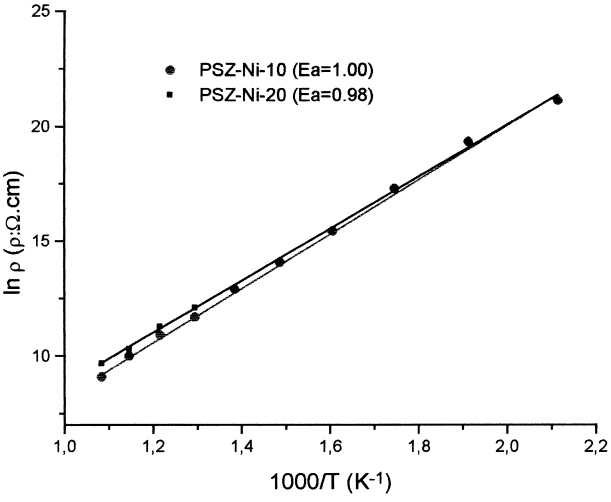

Fig. 9. Electrical resistivity as a function of temperature for PSZ–Ni.

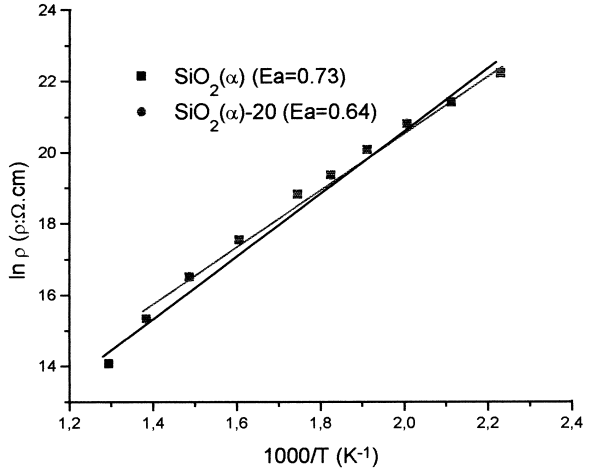

Fig. 10. Electrical resistivity of cristobalite nominally pure and containing 20 vol% Ti as a function of temperature.

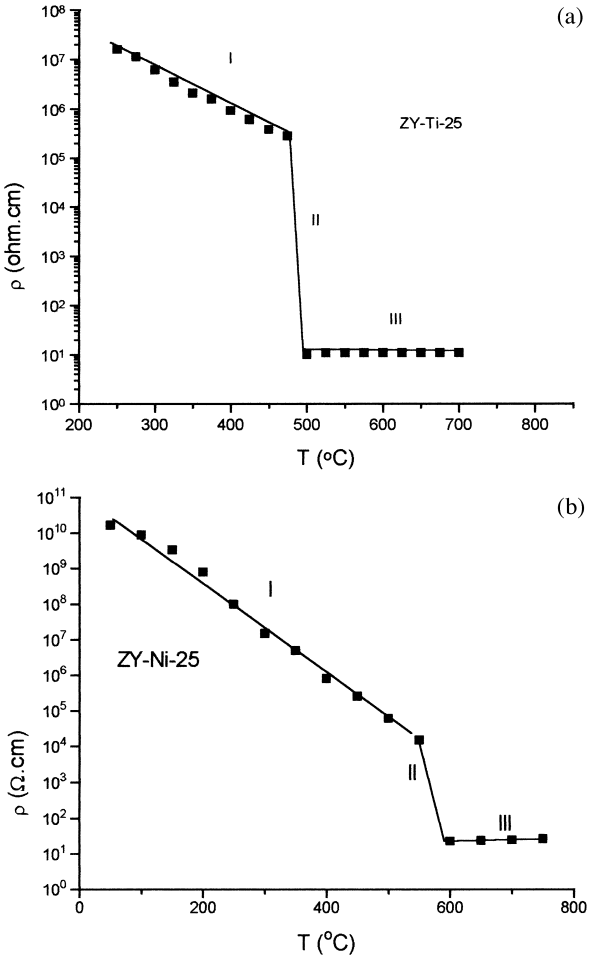

Fig. 11. Electrical resistivity as a function of temperature for: (a) PSZ–Ti; and (b) PSZ–Ni containing 25 vol% of metallic inclusions.

estimated. As the temperature is raised the metallic inclusion fraction volume reaches the critical fraction and the metallic particles touch themselves forming conduction paths. PSZ–Nb samples do not show this behavior because the thermal expansion coefficients of PSZ and Nb are close.

Fig. 12 shows the electrical resistivity as a function of temperature for a cristobalite 30 vol% Ti.

As can be seen there are again three distinct regions corresponding to the resistivity behavior. In region I the resistivity increases linearly as the temperature is raised. In region II there is a sharp increase of resistivity indicating that a percolation phenomenon is occurring. In region III the resistivity decreases exponentially as the temperature is raised. The activation energy in this region is 0.63 eV. The conduction mechanisms can be assumed to be similar to the ones related to pure cristobalite.

The volumetric fraction of metallic inclusions in cristobalite samples containing 30 vol% of Ti reaches values lower than the critical fraction as the temperature is raised because there is a phase transformation of cristobalite at 250°C and consequently 1.6 % volume change. In the case of metal–metal and metal–semiconductor, when particles touch themselves, space charges are created and the Fermi energies are equilibrated. The migration of charge carriers from one material to the other leads to energy band distortion, and as a consequence, some electrons (or holes) can occupy energy states in the conduction band (or valence band), and migrate through the material by percolation. The percolation through touching metal particles is not identical with that through overlapping space charge layers [12]. In the present work, metal particles are in contact with insulators, which present higher energy gaps between valence and conduction bands. Therefore, even if the bands are distorted close to the particle surfaces, there are no conclusive evidences that layers of space charge could be overlapping to promote percolation. As the temperature is raised, phase changes could change the space charge distribution, but a more detailed study is required to produce stronger evidences of this phenomenon.

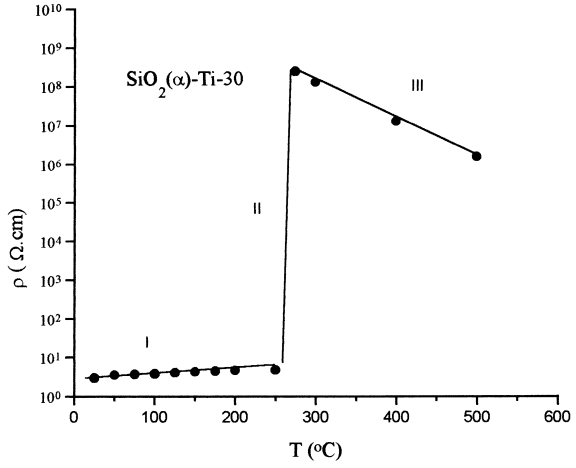

Fig. 12. Electrical resistivity as a function of temperature for αSiO_2–Ti 30.

6. Response of samples exposed to r.f.

Fig. 13 shows the surface temperature of PSZ samples containing 30 vol% of Ti, Nb or Ni, and a cristobalite sample containing 30 vol% during the exposition to electromagnetic fields in the range of r.f. as a function of voltage applied in the induction coil.

The asymptotic behavior of temperatures for the highest voltage values is due to the heat loss caused by radiation, convection or even conduction. This loss depends on the forth power of temperature [17]. To reach higher temperatures, this loss should be reduced.

In order to compare the response of each material, temperatures were measured for each material by fixing the induction coil voltage to 0.4 kv. Table 3 shows these results.

Different materials responsiveness can be explained considering that the temperature is proportional to the parasitic current induced inside the material. In the other hand the current flow is proportional to the material electrical conductivity and magnetic permeability. As the electrical resistivity at room temperature for Ti, Nb, and Ni are 47.8×10^{-6}, 15.2×10^{-6} and 6.84×10^{-6} Ω cm respectively, materials with higher resistivity will reach lower temperatures as shown in Table 3. In the other hand, Ni shows higher magnetic permeability and that helps its response to electromagnetic fields.

The temperature reached by PSZ–Ti is slightly higher than the one reached by SiO_2–Ti because the ionic conductivity of PSZ is also higher than the one for cristobalite, and therefore, the charge carrier concentration would be higher for PSZ–Ti than for cristobalite–Ti. Samples containing metallic inclusions lower than 30 vol% do not self-heat considerably when exposed to r.f. because the parasitic currents are very low.

Considering that the Ti density is lower than that of PSZ and in the present work the Ti average particle size

Table 3
Temperature values for composites containing 30 %vol of metallic inclusions

Material	Temperature (°C)
PSZ–Ti	1130
PSZ–Nb	1190
PSZ–Ni	1500
SiO_2–Ti	1100

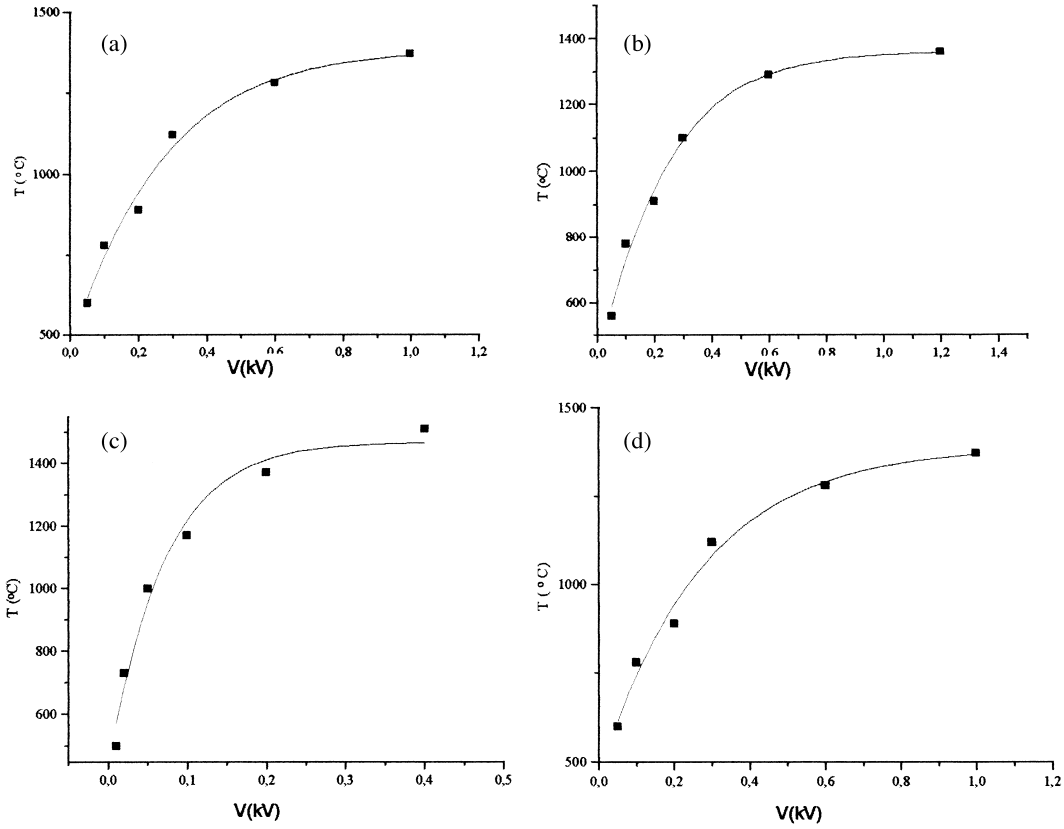

Fig. 13. Surface temperature as a function of electric tension (V) for: (A) PSZ–Ti; (B) PSZ–Nb; (C) PSZ–Ni; and (D) SiO_2–Ti . The samples contained 30 vol% of metallic inclusions.

is lower than the PSZ ones, it was assumed that a better slurry could be obtained and crucibles of PSZ–30 vol% Ti and PSZ 35 vol% Ti were made by slip casting. By fixing the power of the induction furnace to 2 kw, these crucibles were tested for self-heating. The maximum temperature reached was 1350°C without charge. Higher temperatures could be reached by improving the inductive coupling, consequently improving the material response.

7. Conclusions

Ceramic matrix composites with electrical conducting paths have been produced by embedding Ti, Nb, and Ni particles in a PSZ or cristobalite matrix. For PSZ with metallic concentrations above 25 vol%, electronic conducting paths have been observed. These paths are generated by touched metallic clusters.

The oxidation of the original metallic particles during the material processing leads to different microstructure characteristics, electrical resistivity and activation energies for electrical conduction. PSZ samples containing Nb or Ni show lower ionic conductivity when compared to nominally pure ones. PSZ containing Ti shows similar ionic conductivity when compared to PSZ nominally pure.

Composite materials made of cristobalite–Ti, as well PSZ containing amounts of Nb, Ti or Ni higher than 25 vol% can self-heat when exposed to electromagnetic fields. Samples of PSZ–Ni showed the best performance concerning the self-heating effect, but the application of this material is limited to the relatively low Ni melting point.

Crucibles of PSZ containing amounts of Ti higher than 25 vol% were made by slip casting. They were checked for self-heating under the exposition of r.f. The maximum temperature reached was 1350°C limited by the heat loss. No visible mechanical damage has been observed after several heating cycles.

Acknowledgements

The authors thank Ms. C. Yamagata, Ms. C. Menezes, and Mr. W. Ussui for helping in the synthesis of PSZ, and Ms. M. Löw for helping with the X-ray diffraction analyses. The Brazilian National Research Council (CNPq) is acknowledged for granting a scholarship and FAPESP for supporting one of the authors.

References

[1] P. Ettmayer, W. Lengauer, The story of cermets, Powder Metall. Int. 21 (20) (1989) 37.

[2] K.K. Chawla, Composite Materials, 2nd ed., Springer–Verlag, New York, 1987.

[3] G. Brauchotte, G. Cizeron, Sintering of alumina–titanium powder mixtures and elaboration of the corresponding cermets, J. Mater. Sci. 24 (1989) 3123.

[4] E. Barbier, F. Thevenot, Electrical resistivity in the titanium carbonitride–zirconia system, J. Mater. Sci. 27 (1992) 2383.

[5] J.R. Martinelli, S.T. dos Reis, Electrical caracterization of zirconia–niobium and zirconia–titanium composites, in: Ceramic Transactions, Vol. 38, Advances in Ceramic–Matrix Composites, 1993, p. 521.

[6] A.M. Anthony, High temperature applications of zirconia, in: A.H. Heuer, L.W. Hobbs (Eds.), Science and Technology of Zirconia, Vol.1, 1981, p. 147.

[7] D.W. Fang, T. Xu, D. Qing, Positive temperature coefficient of resistance effect in hot-pressed cristobalite — silicon carbide composites, J. Mater. Sci. 29 (1992) 1097.

[8] G. Hohenberger, G. Tomandl, R. Ebert, T. Taube, Inhomogeneous conductivity in varistor ceramics: methods of investigation, J. Am. Ceram. Soc. 74 (9) (1991) 2097.

[9] J. Koger, C.E. Holcomber, J.G. Banker, Coating on graphite crucibles used in melting uranium, Proceedings of the International Conference on Metallurgical Coating: Thin Solid Films, 5–8 April 1976, San Francisco, CA, p. 297.

[10] R.C. Garvie, R.H.J. Hannink, M.V. Swain, X-ray analysis of transformed zone in partially stabilized zirconia (PSZ), J. Mater. Sci. Lett. 1 (1982) 437.

[11] F. F. Sene, Electrical resistivity of ceramic–metal composite materials in the percolation region, application in crucibles for induction furnaces, Master thesis, IPEN — University of Sao Paulo, 1997.

[12] J. Kieffer, J.B. Wagner Jr., Electrical conductivity of metal–metal oxide composites, J. Electrochem. Soc. 135 (1988) 1.

[13] R. Landauer, The electrical resistence of binary metallic mixtures, J. Appl. Phys. 23 (1952) 779.

[14] C.R. Barret, W.D. Nix, A.S. Tetelman, The Principle of Engineering Materials, Prentice-Hall, Englewood Cliffs, NJ, 1973.

[15] P. Kofstad, Nonstoichiometry, Diffusion and Electrical Conductivity in Binary Metal Oxides, Wiley Interscience, New York, 1972.

[16] O. Sudre, F.F. Lange, Effect of inclusions on densifications, J. Am. Ceram. Soc. 75 (1) (1992) 519.

[17] H. Sobokta, Equipos Industriales para Calentamiento por A.F., Paraninfo, Madrid, 1968.